Radioprotection 2018, 53(1), 27–31
© EDP Sciences 2018
https://doi.org/10.1051/radiopro/2017041

Available online at:
www.radioprotection.org

ARTICLE

Selective contribution of concrete shielding on the equivalent and effective doses in a prostate radiotherapy treatment

K.L. Braga[1], J.L. Thalhofer[2], W.F. Rebello[1,3], R.G. Gomes[1,2], M.P.C. Medeiros[2], H.C. Vital[1], A.X. Silva[2] and E.R. Andrade[1,4,5,*]

[1] Nuclear Engineering Graduate Program, Military Institute of Engineering, (IME), Rio de Janeiro, Brazil.
[2] Nuclear Engineering Graduate Program, Federal University of Rio de Janeiro (COPPE/UFRJ), Rio de Janeiro, Brazil.
[3] Rio de Janeiro State University, Faculty of Engineering, and IBRAG, Rio de Janeiro, Brazil.
[4] Institute of Radioprotection and Dosimetry (IRD), Rio de Janeiro, Brazil.
[5] IBMEC-RJ, Engineering Faculty, Rio de Janeiro, Brazil.

Received: 7 January 2017 / Accepted: 19 December 2017

Abstract – Within a radiotherapy room, in addition to the primary beam, there is also secondary radiation that leaks from the accelerator head and scattering caused by surrounding objects, the patient's body and even the walls of the shielded room itself, designed to protect the external individuals, disregarding effects on the patient. The aim of this work is to study the radiation effect on the patient's healthy tissues caused by scattering from a concrete shield expressed as equivalent and effective doses. MCNPX simulations of the linear accelerator Varian 2100/2300C/D were performed for a MAX phantom of a patient in a typical radiotherapy room. In addition, calculations were made with and without shielding. It was concluded that the concrete shielding affects in 5% the effective dose absorbed by the patient.

Keywords: dose equivalent / effective / shielding / radiation therapy

1 Introduction

Doses of ionizing radiation and their biological effects are parameters that lead to protocols in radiotherapy. Thus, both doses as well as their distribution must be known so as not to compromise quality and safety. In radiotherapy using linear accelerators, the problem becomes more relevant at higher energies, with the possibility of photoneutrons being generated when energies above 6 MeV are used. Since the 1970s, some studies have been focused on the investigation of radiation transmission in concrete and secondary radiation production by using accelerators (Tochilin and LaRiviere, 1979; LaRiviere, 1984; Shobe *et al.*, 1999). On the other hand, those studies do not consider the contribution of the shielded walls to the doses (equivalent/effective) absorbed by the patient. Thus, any initiative that would reduce the dose, not only to the patient but also to the public, should be regarded as a contribution to optimize radiation protection and environmental control procedures.

To reduce the contribution from scattered radiation, there has been a considerable increase in research effort devoted to the development of specific materials and their combinations. The purpose of such studies is thus to develop an improved shielding (Mutic *et al.*, 2001; NCRP, 2005), considering that secondary radiation is typically contributed by:

- leakage in the linear accelerator head;
- the scattering caused by neighboring objects;
- the patient's body;
- by surroundings (walls, floor and ceiling).

It should be considered that standards for radiotherapy establishing minimum requirements for shielding are addressed to occupationally exposed individuals and the public protection not the patient.

According to the ALARA principle, *As Low As Reasonably Achievable*, the dose absorbed by the patient should always be minimized as a result of safe practices (Xu *et al.*, 2008; Fasso and Rokni, 2009), consequently reducing the risk of secondary morbidities. Thus, shielding calculations performed with the Monte Carlo code remain as an important tool to ensure safety.

The objective of this work is to perform Monte Carlo calculations to investigate the effects of scattered radiation (photons and neutrons) by concrete shielding over healthy tissues, expressed as equivalent (tissues/organs) and effective (patient) doses during treatment for prostate cancer.

*Corresponding author: fisica.dna@gmail.com

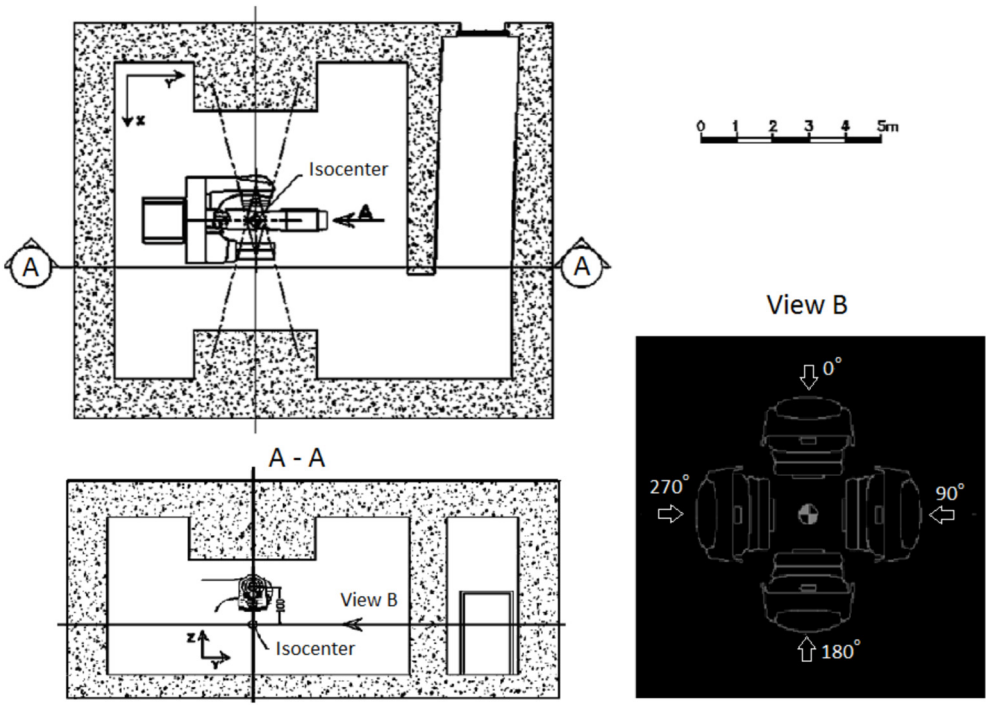

Figure 1. Plan and section view of the radiation therapy room including the gantry inclination angles (view B) used in the simulation.

2 Methodology

The Monte Carlo N-Particle eXtended version 2.7.0 – MCNPX (Pelowitz, 2011) code was used for modeling a standard radiotherapy room including radiation scattered from surroundings (that include its concrete walls, floor and ceiling). MCNPX enables the simulation of several types of radiation, such as photons and neutrons. Also, it is possible to simulate varied types of interaction such as incoherent and coherent scattering, fluorescent emission after photoelectric absorption, pair production with local emission of annihilation photons, bremsstrahlung and, production of neutrons (Jeraj *et al.*, 1999). A Varian linear accelerator 2100/2300C/D operating at 18 MV was considered in all simulations. A treatment of prostate cancer 3DCRT under four fields was considered in two situations, with and without surroundings, was used to simulate the patient's body. Values for equivalent and effective doses absorbed by the patient calculated for each situation were compared to evaluate the influence caused by the surroundings on the final radiation equivalent and effective doses throughout the treatment. Prostate cancer was chosen because it is a very common type of cancer.

Modeling was performed assuming operation of the linear accelerator at 0°, 90°, 180° and 270° as recommended for prostate cancer treatment according to the Brazilian Institute for Cancer – INCA protocol and the walls of the room were assumed to be made of concrete with density of 2.35 g cm^{-3} (Kase *et al.*, 2003; NCRP, 2005) and composition described in Table 1 (Kase *et al.*, 2003). Photon and neutron equivalent and effective doses were calculated for each gantry angle for both cases (with and without surroundings). For the accelerator, the use of MLC 120 was considered, with the opening fields of jaws and MLC defined to allow irradiation of the whole prostate. That feature led to the use of irradiation fields in the order of 9×9 cm^2 on slopes of 0° and 180° and in the order of 7×9 cm^2 at angles of 90° and 270°.

In the calculation of equivalent and effective doses, weight parameters were used for the type of radiation as well as organs and tissues as recommended in ICRP 103 (Weiss, 2009; Sato *et al.*, 2011). The results were normalized relatively to a prostate dose of 1 Gy due to photons. A total of 600 million and 2 billion stories were used in each MCNPx simulation for photons and neutrons, respectively. Estimated statistical uncertainties are less than 5% for tissue/organs near the isocenter and up to 10% further away. Considering organs and tissues positioned near the prostate (isocenter), and less than 10% for thyroid, brain and skull. In the calculation of the effective dose, the portion of the dose deposited in the prostate was not considered since the interest of the study is specifically in the healthy tissues of the patient, besides being that the target organ, the extremely high dose would mask the dose contribution in the other organs.

It was considered in this study that the radiotherapy room is located on the ground floor of a building, containing a primary armor belt positioned on the walls and ceiling, with thicknesses of 2.45 m and 2.10 m respectively and on the floor only one slab. In the plan, the isocenter is positioned in the middle of the distance of the inner faces of the primary belt, exactly 3.05 m of them and, in cut, at a distance of 1.75 m from the underside of the ceiling shield and at a distance of 1.33 m from the top face of the floor. Figures 1 and 2 show: (1) the plan and section view of the radiation therapy room, (2A) perspective views showing the model of the phantom and (2B) a general view of the model created from MCNPX. Table 1 shows Bunker's modeling concrete constitution. The images shown in Figure 1 and 2A were obtained through the AutoCAD program, used as an aid in the previous study of the geometry of the radiotherapy room and the head. Except for the head casing, merely

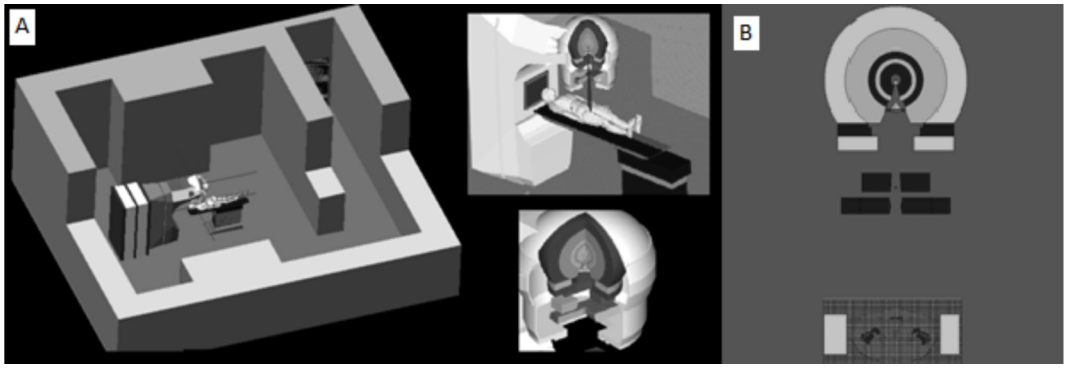

Figure 2. A: represents a perspective view showing the model of the phantom, the accelerator and the radiotherapy room. Also shown in detail are the modeling of the phantom, of the accelerator, and of the head of the accelerator. The housing surrounding the equipment head is merely illustrative and has not been simulated. B: represents a general view of the modeled accelerator obtained by the Visual Editor, where the accelerator head can be observed at zero degrees and a longitudinal and cross section of the phantom, left and right images, respectively.

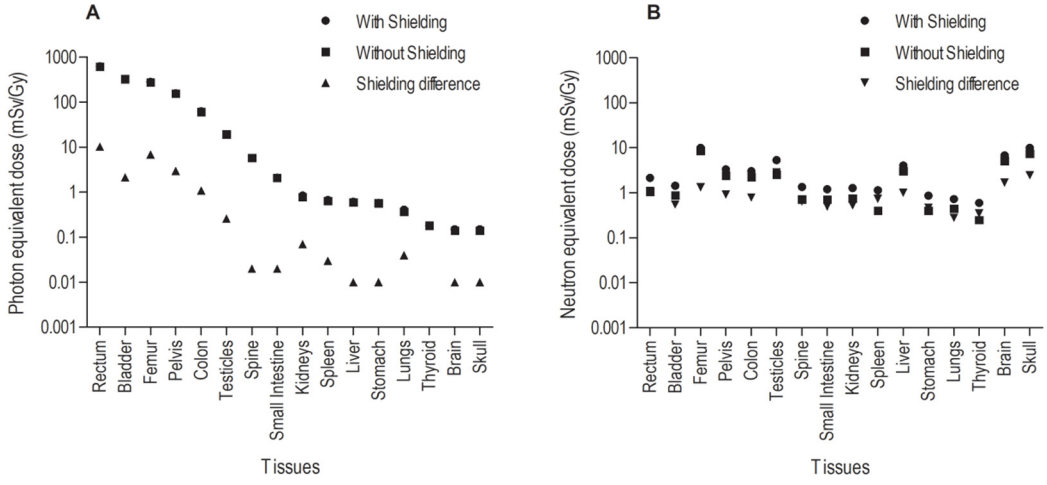

Figure 3. Direct and scattered radiation contributions to the equivalent doses. A: equivalent dose due to photons. B: equivalent dose due to neutrons.

illustrative (white). The table, patient and, the image faithfully represents what was modeled in the MCNPX. The image shown in Figure 2B was created by Visual Editor software.

For the photonuclear interactions, the la150 shock-drying library was used. For the nuclides not included in this library, the physical model CEM03 was used.

3 Results

Figure 3 (A and B) shows the influence of radiation scattered from the surroundings on the equivalent doses absorbed by the patient. It results from the interaction of the primary beam of photons with the walls, floor and ceiling of the treatment room. Figure 3A shows the equivalent dose for the tissues/organs due to photons considering the surroundings while Figure 3B shows the one due to neutrons.

Table 2 presents data for the influence of surroundings on the total equivalent dose (contributed by photons and neutrons) in each tissue/organ. Data are summarized in Figure 3A and B.

Table 3 compares effective doses calculated with and without surroundings due to photons and neutrons. Calculations were performed according to the methodology recommended by ICRP 103 (Weiss, 2009; Pujades Claumarchirant *et al.*, 2010; Sato *et al.*, 2011).

Table 1. Bunker's modeling concrete constitution.

Concrete ($\rho = 2.35$ g cm^{-3})	
Isotope	Mass (%)
^{1}H	0.55
^{12}C	0.48
^{16}O	49.57
^{27}Al	4.55
^{28}Si	31.36
^{40}Ca	8.26
^{56}Fe	1.23
^{23}Na	1.70
K_{nat}	1.91
Mg_{nat}	0.26
S_{nat}	0.13

Table 2. Total contribution of shielding due to photons and neutrons.

Tissues	Total normalized equivalent dose (mSv Gy^{-1})		Total surroundings contribution	
	With surroundings	Without surroundings	mSv Gy^{-1}	%
Femur	293.12	284.93	8.19	2.79
Inf bone leg	8.2	6.4	1.8	21.95
Tibia and fibula	15.06	11.47	3.59	23.84
Prostate	1001.16	1001.05	0.11	0.01
Pelvis	161.31	157.43	3.88	2.41
Testicles	24.91	21.86	3.05	12.24
Rectum	629.3	617.87	11.43	1.82
Colon	65.65	63.77	1.88	2.86
Stomach	1.45	0.97	0.48	33.10
Small intestine	3.31	2.79	0.52	15.71
Spleen	1.81	1.04	0.77	42.54
Pancreas	1.47	1.22	0.25	17.01
Kidneys	2.13	1.53	0.6	28.17
Bladder	328.48	325.78	2.7	0.82
Liver	4.67	3.65	1.02	21.84
Esophagus	1.63	1.02	0.61	37.42
Lung	1.14	0.82	0.32	28.07
Thoracic region	4.1	2.79	1.31	31.95
Humerus	7.88	6.05	1.83	23.22
Skin	26.85	21.26	5.59	20.82
Average skeleton	51.18	48.5	2.68	5.24
Muscle	35.33	32.93	2.4	6.79
Cartilage	18.12	14.16	3.96	21.85
Adipose	39.93	36.85	3.08	7.71
Remaining	34.75	32.21	2.54	7.31
Thymus	1.29	0.83	0.46	35.66
Trachea	1.61	0.83	0.78	48.45
Thyroid	0.78	0.43	0.35	44.87
Gl. Adrenal	1.34	0.61	0.73	54.48
Brain	6.96	5.27	1.69	24.28
Skull	10.05	7.57	2.48	24.68
Spine	7.16	6.5	0.66	9.22
Jaw	10.56	8.75	1.81	17.14
Eye's lens	25.25	18.2	7.05	27.92

Table 3. Comparison of calculated values of effective dose with and without surroundings.

Tissues	Effective Dose (ED) (mSv Gy^{-1})					
	With surroundings			Without surroundings		
	ED $_{photons}$	ED $_{neutrons}$	ED $_{Total}$	ED $_{photons}$	ED $_{neutrons}$	ED $_{Total}$
Effective dose	26.3941	3.0048	29.3989	26.0768	1.9547	28.0315

4 Discussion

Based on the calculations, it can be concluded that there was important contribution from photons scattered in the surroundings to the equivalent dose even when tissues/organs further away from the primary beam (Fig. 3A) were considered. Compared to photons, neutrons have a lower contribution to the equivalent dose for tissues at sites close to the isocenter as can be concluded from the analysis of Figure 3A and B. However, neutron contribution, although smaller than that from photons, seems to be space independent, being practically the same for all tissues/organs, except at the isocenter, where the dose due to neutrons can be neglected. This finding could be explained by the contribution of neutrons produced isotropically in the photonuclear reaction.

That also implies that in a treatment of prostate cancer with 74 Gy of total therapeutic dose, for instance, the surroundings would add 100 mSv to the patient's effective dose not accounting for the prostrate contribution. Such figure is the dose accounted as the limit for emergency response considering whole-body exposure (Mettler, 2012). It can be noticed that the increase in effective dose on the patient corresponds to 78% from neutrons and 23% from photons contribution.

Thus, a material that efficiently absorbs neutrons radiation in the room might impact the effective dose significantly. For future studies, an additional layer of material with high neutron absorption cross section should be added to the walls to reduce the effective dose absorbed by the patient.

Based on the MCNP calculations performed in this work, it was possible to conclude that the dose from scattered radiation, although relatively small, is by no means negligible. That finding should be taken in consideration in the design of safer radiotherapy rooms. Thus, minimizing scattered dose should be of great concern in order to protect the health of patients and further efforts should be made in order to ensure that a level of stray radiation as low as reasonably achievable be pursued in radiation therapies.

5 Conclusion

Analysis of the calculated data allows us to conclude that the concrete walls of the standard radiotherapy room (surroundings) contribute with approximately 5% of the effective dose absorbed by the patient in prostate treatment. Therefore, these doses on the patient should not be disregarded in the room shielding calculation methodologies. Ongoing studies are now focused on the assessment of:

- implementation of experimental measures to compare and evaluate the quality of the results obtained in the simulation;
- risk factors calculation for secondary cancer in healthy tissues based on improved estimates of scattered radiation;
- the efficiency of a layer of a neutron absorbing material to be added to the walls in order to reduce the flux of backscattered radiation and its negative effects;
- treatment of the tumor in other tissues;
- use of other linear accelerators operating at other energies;
- use of other treatment techniques such as IMRT.

This work is expected to draw attention to the problem of radiation production and scattering within radiotherapy rooms and their effects on patients. In addition, it is expected that future studies can be motivated in order to improve shielding calculations as well as the selection of more suitable materials that could reduce doses to patients.

Finally, it is important to emphasize that this work represents a preliminary study in which the dose contribution on the patient due to the screening of the room is suggested under limited information. These limitations are mainly addressed to the lack of performing experimental measurements to compare and to model a single cancer treatment protocol without variations in geometry, accelerator energy, and shielding materials.

References

Fasso A, Rokni S. 2009. Operational radiation protection in high-energy physics accelerators: implementation of ALARA in design and operation of accelerators, *Radiat. Prot. Dosim.* 137(1–2): 94–99.

Jeraj R, Keall PJ, Ostwald PM. 1999. Comparisons between MCNP, EGS4 and experiment for clinical electron beams, *Phys. Med. Biol.* 44(3): 705–717.

Kase KR, Nelson WR, Fasso A, Liu JC, Mao X, Jenkins TM, Kleck JH. 2003. Measurements of accelerator-produced leakage neutron an photon trasmission through concrete, *Health Phys.* 84(2): 180–187.

Kramer R, Vieira JW, Khoury HJ, Lima FR, Fuelle D. 2003. All about MAX: a male adult voxel phantom for Monte Carlo calculations in radiation protection dosimetry, *Phys. Med. Biol.* 48(10): 1239–1262.

LaRiviere PD. 1984. Transmission in concrete of primary and leakage X-rays from a 24-MV medical linear accelerator, *Health Phys.* 47(6): 819–827.

Mettler FA. 2012. Medical effects and risks of exposure to ionising radiation, *J. Radiol. Prot.* 32(1): N9–N13.

Mutic S, Low DA, Klein EE, Dempsey JF, Purdy JA. 2001. Room shielding for intensity-modulated radiation therapy treatment facilities, *Int. J. Radiat. Oncol. Biol. Phys.* 50(1): 239–246.

NCRP (2005). NCRP – Report n° 151: Structural shielding design and evaluation for megavoltage X- and gamma-ray radiotherapy facilities. Washington, D.C., NCRP – National Council on Radiation Protection and Measurements.

Pelowitz DB. 2011. MCNPX^{TM} user's manual. LA-CP- 11–00438.

Pujades Claumarchirant MC, Marti Vidal JF, Olivas Arroyo C, Bello Arques P, Mateo Navarro A. 2010. Application of ICRP-103 in the calculation of effective dose associated to nuclear medicine tests, *Rev. Esp. Med. Nucl.* 29(3): 114–121.

Sato T, Endo A, Yasuda H, Niita K. 2011. Impact of the introduction of ICRP Publication 103 on neutron dosimetry, *Radiat. Prot. Dosim.* 146(1–3): 183–185.

Shobe J, Rodgers JE, Taylor PL. 1999. Scattered fractions of dose from 6, 10, 18, and 25 MV linear accelerator X-rays in radiotherapy facilities, *Health Phys.* 76(1): 27–35.

Tochilin E, LaRiviere PD. 1979. Attenuation of primary and leakage radiation in concrete for X-rays from a 10 MV linear accelerator, *Health Phys.* 36(3): 387–392.

Weiss W. 2009. Towards a coherent conceptual framework for emergency preparedness/response and rehabilitation – the application of the new ICRP recommendations given in ICRP 103, *J. Environ. Radioact.* 100(12): 1002–1004.

Xu XG, Bednarz B, Paganetti H. 2008. A review of dosimetry studies on external-beam radiation treatment with respect to second cancer induction. *Phys. Med. Biol.* 53(13): R193–241.

Cite this article as: Braga KL, Thalhofer JL, Rebello WF, Gomes RG, Medeiros MPC, Vital HC, Silva AX, Andrade ER. 2018. Selective contribution of concrete shielding on the equivalent and effective doses in a prostate radiotherapy treatment. *Radioprotection* 53(1): 27–31